Polarization Modulation Infrared Reflection Absorption Spectroscopy at Elevated Pressures: CO Adsorption on Pd(111) at Atmospheric Pressures

Emrah Ozensoy, Douglas C. Meier, and D. Wayne Goodman*

Department of Chemistry, Texas A&M University, P.O. Box 30012, College Station, Texas 77842-3012

Received: February 26, 2002; In Final Form: July 10, 2002

CO adsorption on a Pd(111) single-crystal surface was investigated using in situ polarization modulation infrared reflection absorption spectroscopy (PM-IRAS) within the pressure range 10^{-6}−800 mbar. The coverage-dependent CO overlayer structures found on the Pd(111) surface are identical throughout this pressure regime, that is, no new surface species at elevated pressures or adsorbate-induced substrate reconstructions were observed. The transition from an adsorbate superstructure dominated by bridged-bound CO to an adsorbate overlayer having 3-fold/atop CO sites was followed by varying the adsorbate pressure over 9 orders of magnitude. The derived phase diagram indicates an apparent activation energy of 44.35 ± 1.63 kJ/mol for the bridged-to-3-fold-hollow/atop transition. A comparison between these data and recent sum frequency generation (SFG) results is made.

I. Introduction

Traditionally, many of the surface science techniques customarily used for investigating heterogeneous catalytic systems require ultrahigh vacuum (UHV) or, at least, pressures much lower than the environments of working technical catalysts.[1] This well-known limitation, the so-called "pressure gap", prevents detailed comparisons between model and technical catalysts.[2,3] However, recently developed in situ vibrational spectroscopic techniques such as sum frequency generation (SFG)[4−7] and polarization modulation infrared reflection absorption spectroscopy[8−14] (PM-IRAS) have provided new means for investigating heterogeneous catalytic systems at or near the pressures of technical catalysts, that is, ambient (atmospheric) pressures. PM-IRAS is a versatile in situ spectroscopic technique that yields vibrational information about the surface species at solid−liquid or gas−solid interfaces by efficiently removing the contribution from the background gaseous species. Elimination of the vibrational features corresponding to the gas-phase species is crucial for the in situ analysis of solid−gas interfaces because the presence of these gas-phase features overwhelms the smaller IR signal of the adsorbed species.

PM-IRAS has been extensively used to study thin polymer films,[15] aqueous adsorbates on copper,[16] in situ electrode−electrolyte surface studies,[14] species at the air−water interface,[8] NO adsorption on Pt,[17] and CO[10] and CO + H_2 coadsorption[11] on Co(0001). The operational principles of PM-IRAS and the associated electronics have been described thoroughly.[8,9,15,18−20] The basic operational principle of the polarization modulation technique is the modulation of a linearly polarized infrared beam by dividing the linearly polarized light into an *s-polarized* beam, which is parallel to the surface of the sample, and a *p-polarized* beam, which is perpendicular to the sample surface. According to the surface selection rules of reflected infrared radiation,[21] species on a metal surface can only absorb *p*-polarized IR light, whereas any molecule in the gaseous or liquid (isotropic) environment can absorb both *p*- and *s*-polarized IR radiation. Therefore, if *s*-polarized absorptions are subtracted from the *p*-polarized absorptions and normalized using the total intensity of both *p*- and *s*-polarized IR beams, a normalized surface-specific IR absorption signal, virtually independent of the environmental conditions, is obtained.

Oxidation of carbon monoxide on Pd surfaces has been a subject of interest for several decades because of its relevance to automotive exhaust emissions.[21] Pd single-crystal surfaces serve as excellent model catalysts for low-pressure surface science studies with respect to the behavior of the more complex technical systems at ambient (atmospheric) conditions. Goodman et al.[22−24] have reported that the surface structure of CO overlayers on Pd(111) single-crystal surfaces follow very similar trends within the pressure range 1×10^{-6} to 13.3 mbar. According to these and related studies,[21,25] the surface structure of CO on Pd(111) depends on the adsorbate coverage. Different CO adsorption sites are occupied within different coverage regimes and a transition from a particular CO phase to another can be altered in a systematic way by manipulating the CO coverage. In this article, we report that the behavior of CO overlayers on Pd(111) single-crystal surface follows virtually identical trends in CO environments from 1×10^{-6} to 800 mbar.

II. Experimental Section

The experiments were carried out in a stainless steel UHV chamber consisting of two compartments. The main chamber was maintained at $<5 \times 10^{-10}$ mbar and equipped with Auger electron spectroscopy (AES), low-energy electron diffraction (LEED), and temperature-programmed desorption (TPD). Attached to the main chamber is an elevated-pressure cell (HPC) equipped with CaF_2 windows. Detailed features of the apparatus can be found elsewhere.[26] The pressure of the HPC could be varied from 5×10^{-12} to 1 bar. The HPC is separated from the UHV chamber via a sliding seal, enabling the transfer of the sample from the UHV chamber to the HPC stage. This arrangement allows sample exposures covering pressures spanning approximately 9 orders of magnitude. The Pd(111) single crystal used in the experiments was spot welded to a Ta wire (0.030 in. diameter). The temperature of the sample was

* To whom correspondence should be addressed. E-mail: goodman@mail.chem.tamu.edu.

10.1021/jp020519c CCC: $22.00
Published on Web 08/20/2002

measured by a W-5%Re/W-26%Re thermocouple spot-welded to the back face of the crystal. Sample temperature was varied from 80 to 1250 K via liquid nitrogen cooling and resistively heating. Pressures within the HPC were measured with a nude Bayard−Alpert-type ionization gauge (Granville-Philips) within the 1.3×10^{-9} to 1.3×10^{-3} mbar range, a 1.3 mbar Baratron gauge (MKS Instruments) within the 1.3×10^{-3} to 1.3 mbar range, and a 1.3 bar Baratron gauge (MKS Instruments) within the 1.3−1333 mbar range.

PM-IRAS spectra were acquired using a Bruker Equinox 55 infrared spectrometer equipped with a water-cooled source. The polarization modulation (PM) optics and the IR spectrometer were located on a steel honeycomb optical top (Technical Manufacturing Corporation), vibrationally isolated with pneumatic legs. PM-IRAS data were acquired at 4.5 min/spectrum (312 scans in the double-sided, forward−backward mode at 4 cm^{-1} resolution) at an angle of 85° from the surface normal. The IR beam leaving the external window of the spectrometer was focused by a Au-coated Al parabolic mirror (focal length 12 in., Bruker Inc.) of which the focal point was coincident with the sample position. The sample was moved into position with respect to the IR beam by a motor-controlled linear transition system on which the analysis chamber is assembled. After reflection from the parabolic mirror, the IR beam passed through a wire-grid polarizer (Graseby Specac, Inc.). Grids of the polarizer were aligned parallel to the sample surface so that the transmitted IR radiation from the polarizer had only a *p*-polarized electric field vector. Linearly polarized light from the wire-grid polarizer was passed through the photoelastic modulation (PEM) optical head (II/ZS50, 50 kHz, Hinds Instruments) with a zinc selenide crystal aligned 45° from the surface normal. The IR beam reflected from the surface was collected by a focusing lens (Bruker, Inc.) and detected by a mercury−cadmium−telluride (MCT) IR detector (D313/6-M, Infrared Associates, Inc.). No purging was used during the PM-IRAS data acquisition, demonstrating the efficiency of the background subtraction. Similarly, the optics were exposed to ambient conditions.

Sum ($p + s$) and difference ($p - s$) signals collected by the detector were processed in real time using a single analogue to digital converter (ADC), a multiplexing electronics unit (IR Multiplexer XA/2,Bruker, Inc.), a photoelastic modulator controller (PEM 90D, Hinds Instruments), and a synchronous sampling demodulator, (SSD-100−15, GWC Instruments). The maximum interferometer velocity that could be achieved by the multiplexer with the described electronics was 10 kHz; therefore, the scanner velocity was set to 10 kHz for PM-IRAS data acquisition. Because the photoelastic modulation efficiency of a linearly polarized IR beam by the zinc selenide crystal is a function of the wavelength of IR light, the PEM controller was set to 1800 cm^{-1} in the half-wave retardation mode to maximize the efficiency of the modulation for a particular temperature and spectral region. The synchronous sampling demodulator was calibrated by adjusting the phases of the sum and difference signals monitored by a dual channel oscilloscope. For each adsorption spectrum, a background PM-IRA spectrum of the clean surface was obtained and the adsorption PM-IRA spectrum was divided by the background spectrum. By this method, the curvature in the initial PM-IRA spectrum due to the second-order Bessel function originating from the photoelastic modulation process was removed. The Pd(111) single crystal was cleaned according to the procedure described by Grunze et al.,[27] and sample cleanliness was checked with AES within the 30−900 eV region. The gas used in the experiments was commercially available research purity carbon monoxide (>99.999%, Matheson-Trigas), which was further purified by cooling in liquid nitrogen. This method allows the cleaning of CO to 600 mbar with the vapor pressure of CO at 90 K. Purification for pressures greater than 600 mbar was carried out using a *n*-pentane/liquid nitrogen slurry maintained at 143 K. The purity of the gas was checked with a quadrupole mass spectrometer (QMS).

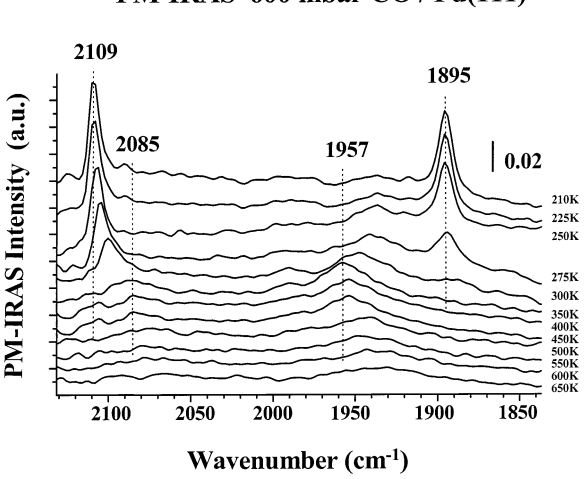

Figure 1. In situ PM-IRAS for CO/Pd(111) in the presence of 600 mbar equilibrium pressure. The spectra were obtained by initially adsorbing CO on Pd(111) at 650 K and decreasing the temperature stepwise to 210 K.

III. Results and Discussion

The coverage-dependent surface structure of CO overlayers on Pd(111) is well-known and has been thoroughly characterized in the literature.[21,25] According to these studies, up to a CO coverage of 0.33 monolayers (ML) on Pd(111), the structure of the adsorbate layer is $(\sqrt{3} \times \sqrt{3})$R30°-1 CO, where the only adsorption sites occupied are the 3-fold hollow sites. Increasing the coverage continuously leads to a new adsorbate structure, at 0.50 ML coverage, the c(4 × 2)-2 CO structure. Although previously[21,25] the bridging sites were suggested to be the only populated adsorption sites at this coverage, recent photoelectron diffraction studies[28] suggest population of the 3-fold sites. Therefore specific site assignments at this coverage are difficult solely on the basis of the vibrational spectroscopic results. As the CO coverage is increased further, the adsorbate structure transforms from c(4 × 2)-2 CO to a (2 × 2)-3 CO structure at a coverage of 0.75 ML. In this configuration, CO molecules populate both the 3-fold hollow sites and the atop sites. The transitions from any of these CO adsorbate structures to another at various temperatures and pressures were presented in a phase diagram by Goodman et al.[22] based on infrared reflection absorption spectroscopy (IRAS) data. In these studies, CO was adsorbed on Pd(111) at pressures ranging from 10^{-6} to 13.3 mbar and the surface coverage of the COwas controlled by varying the surface temperature. Figure 1 shows PM-IRAS data for CO on Pd(111) obtained in situ with a CO pressure of 600 mbar in equilibrium with the surface.

For the series of spectra in Figure 1, CO was dosed to the Pd(111) surface at 650 K with increasingly higher exposures to that corresponding to an equilibrium pressure of 600 mbar. Then the sample temperature was decreased to the indicated values, and in situ PM-IRAS was acquired. Accordingly, the spectra were obtained from the low-coverage to the high-

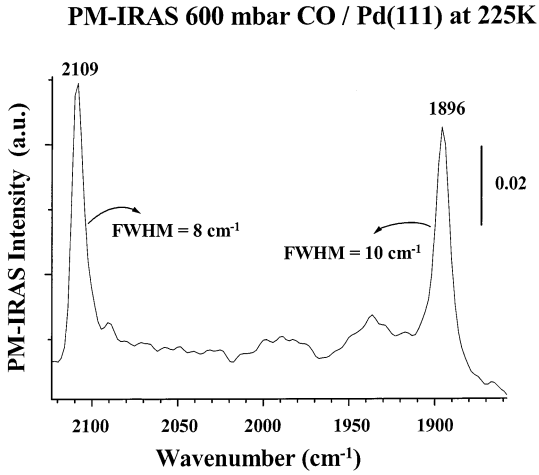

Figure 2. Peak features for the in situ PM-IRA spectrum of 600 mbar CO/Pd(111) at 225 K.

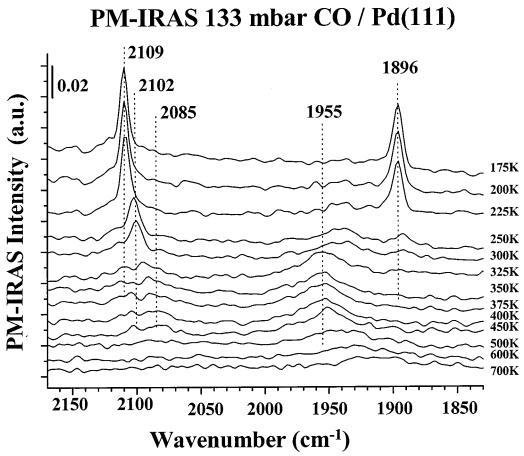

Figure 3. 3. In situ PM-IRA spectrum of 133 mbar CO on Pd(111). Each spectrum was obtained at the given temperature. Initial dosing was at 700 K.

coverage regime. At a sample temperature of 650 K, a broad feature appearing at about 1933 cm^{-1} was observed. As discussed above, this feature can be assigned to the C−O stretching feature associated with the CO molecules located on either the bridging[21] or 3-fold sites[28] on the Pd(111) surface. As the CO coverage is increased by decreasing the temperature, this broad feature sharpens and shifts to a higher frequency at 1957 cm^{-1}, consistent with a more-ordered adsorbate superstructure in which only the bridging sites are occupied. A further increase in the adsorbate coverage leads to a red frequency shift in this feature, as well as a reduced peak intensity. In addition, growth of a feature at ∼2085 cm^{-1}, as well as a second feature at 1895 cm^{-1}, is apparent. These features are associated with CO molecules adsorbed on atop and 3-fold hollow sites on the Pd(111) surface, respectively.[21] In addition, a weak feature near 1990 cm^{-1} was detected between 500 and 275 K. As the surface coverage is further increased, disappearance of the feature at 1936 cm^{-1} and, concurrently, the growth of the atop and 3-fold hollow features are observed. The vibrational frequency shifts of the feature observed within ca. 1930 and 1960 cm^{-1} can be explained by considering the dynamic behavior of the CO adsorption sites with respect to the CO coverage. In the low-coverage regime (T > 500 K), CO can occupy mostly 3-fold sites, which results in a C−O stretching frequency near 1930 cm^{-1}. With increasing coverage ($T \approx$ 350 K), CO molecules move toward the bridging sites resulting in a higher vibrational frequency, which is representative of the bridging sites (i.e., 1957 cm^{-1}). As the coverage is increased further, a phase transformation from bridging to atop/3-fold sites shifts the CO frequency to a lower value.

It is noteworthy that the vibrational frequency of the 3-fold hollow sites remains almost constant during the formation of the (2 × 2)-3 CO adsorbate structure, whereas the vibrational frequency of the atop sites shifts to a higher frequency (from 2085 to 2109 cm^{-1}). This can be because during the phase transition from c(4 × 2)-2 CO to (2 × 2)-3 CO, CO bound to the 3-fold sites may be more rigid with respect to the substrate than is CO bound to atop sites. In the case of (2 × 2)-3 CO overlayer, the full width at half-maximum (fwhm) of the atop and 3-fold peaks were determined to be 8 and 10 cm^{-1}, respectively (see Figure 2).

These sharp features seen in Figure 2 can be regarded as an indication of the stable and well-ordered Pd(111) surface, which does not go through an adsorbate-induced reconstruction at elevated pressures. Such an adsorbate-induced surface reconstruction was suggested in the literature[5] for high-pressure CO adsorption on Pt(111) surface due to the significant broadening of the CO vibrational bands with increasing pressure. It should be noted that the weak features at 1933 and ∼1990 cm^{-1} in Figure 2 are most likely due to the slight disorder in the (2 × 2)-3 CO overlayer in which some of the CO molecules reside on the locations that are between bridge−atop and bridge−3-fold sites or due to CO molecules that are located at the anti-phase domain boundaries with a higher local CO coverage than the overlapping domains. In the literature,[29] a local high coverage in the anti-phase domain boundaries resulting in a strong repulsion between CO molecules was proposed to be the reason for a C−O stretching frequency at ca. 1940 cm^{-1} on Pd(111). In addition, the feature at 1933 cm^{-1} was also observed by Kuhn et al.[22] at 90 K at ∼10^{-6} mbar CO pressure (as well as the expected features at 1894 and 2110 cm^{-1} of the ordered (2 × 2)-3 CO overlayer) by initially dosing CO at temperatures below 600 K and thus preventing the ordering of the CO overlayer. It should also be mentioned that when the CO overlayer shown in Figure 2 is annealed to a higher temperature and cooled to 210 K, the features at 2109 and 1895 cm^{-1} are observed to become sharper with a decrease in the intensity of the weak features at 1933 and 1990 cm^{-1}. This irreversibility of the spectrum in Figure 2 with respect to temperature argues against assigning the feature at 1990 cm^{-1} to a CO species bound to a defect site (as such a feature was observed to be the dominant feature for a defect-rich Pd(111) surface and assigned to CO bound to a bridge site on a step edge[30]), which could have been formed after an adsorbate-induced surface reconstruction at high pressures. The same set of experiments were performed at different equilibrium CO pressures to verify the correlation between the behavior of the Pd(111) surface at high and low adsorbate pressures. Figure 3 shows an isobaric set of PM-IRAS data collected at 133 mbar CO. Comparison of Figure 1, Figure 3, and other lower-pressure results (not shown here) show that the structure of the CO overlayer changes insignificantly within the 10^{-6}−800 mbar region, that is, no high-pressure-induced CO species on Pd(111) were observed.

Recently, similar high-pressure experiments on the CO/Pd(111) system using SFG have been reported by Rupprechter and co-workers[30−32] within the 10^{-8}−1000 mbar region. SFG results presented in these studies correlate very well with the current PM-IRAS results. However, important differences between the SFG and PM-IRAS results are noteworthy. One of the most striking differences is the gross underestimation of

the 3-fold hollow sites (~1895 cm^{-1}) by the SFG technique. In these studies, the CO signal detected for the 3-fold sites is significantly smaller than that for the atop sites. However, in the PM-IRAS results at coverages near 0.75 ML, the total peak area of the feature due to CO bound at 3-fold hollow sites is about 95% of the peak area associated with the atop sites. This 1:1 ratio of the signals arising from CO bound at atop and 3-fold hollow sites measured in the PM-IRAS experiments more closely approximates the estimated (2 × 2)-3 CO overlayer structure[21] at 0.75 ML coverage, in which the number of atop sites is half the number of 3-fold sites. The remaining discrepancy between the measured ratio and the true ratio likely stems from two physical considerations common to all IRAS experiments. First, the integrated intensity of any infrared absorption band is proportional to the square of the dynamic dipole moment of the oscillator.[21] Given the different environments for CO bound at atop versus 3-fold hollow sites, it follows that the dynamic dipole moments for the transitions may be different as well. This is especially plausible considering the ~200 cm^{-1} difference between the two frequencies. The other factor likely affecting the absorption intensity is dipole−dipole interaction of equivalent parallel oscillators on the surface.[33] This effect tends to attenuate infrared absorption intensity as the population of neighboring equivalent dipoles increases; because of their higher population, it is expected that absorbance features attributed to CO at 3-fold hollow sites would experience greater attenuation.

Rupprechter et al.[30,31] reported that the spectral region below 1900 cm^{-1} could not be studied as effectively with SFG because of instrumental limitations particular to their study. PM-IRAS, on the other hand, enables investigation over the spectral window ~2100−1400 cm^{-1} even at quasi-atmospheric pressures; in addition, this spectral window can be routinely adjusted to encompass any desired window of similar bandwidth by simply changing the photoelastic modulator frequency to whatever value is optimum for the desired spectral window. Furthermore, asymmetry in the line shapes of the SFG data was not observed in the PM-IRAS results in which the IR absorption features are relatively symmetric (Lorentzian-type). In addition, at high-pressure conditions, it was pointed out[31] that in SFG significant loss in the incoming IR laser intensity due to gas-phase species leads to a significant decrease in the atop CO intensity above 500 mbar of CO(g). This result was attributed[31] to the inaccuracy of the calibration method that was used to account for the changes in the incoming IR intensities. PM-IRAS effectively acts as a double-beam experiment wherein the gas-phase interference is removed from the spectrum with minimal error. Loss of spectral intensity in the region of the CO gas-phase envelope only becomes critical as the CO pressure is increased sufficiently to become opaque to infrared radiation within the frequency envelope of the gas-phase spectrum. A comparison of the PM-IRAS results presented in Figures 1 and 3 shows no decrease in the atop CO peak intensities with an increase in pressure from 133 to 600 mbar, although a decrease in the S/N was observed in the higher-pressure case (i.e., at 600 mbar) due to the larger infrared absorption of the gas-phase species with respect to the surface species

Using the high-pressure data that were obtained in this study, we can extend the phase diagram previously reported by Goodman et al.[22] for the transition from the bridging CO overlayer structure to the 3-fold hollow/atop structure below 13 mbar to higher pressures. Figure 4 shows this phase diagram with the additional high-pressure data. The linearity of the Arrhenius plot even at elevated pressures (close to atmospheric pressures) is apparent. A Clausius−Clapeyron activation energy of 44.35 ± 1.63 kJ/mol was derived from the slope of the plot; a value close to 39.8 kJ/mol was derived for the phase transition from bridging to 3-fold hollow CO structures using temperature-programmed desorption results.[22]

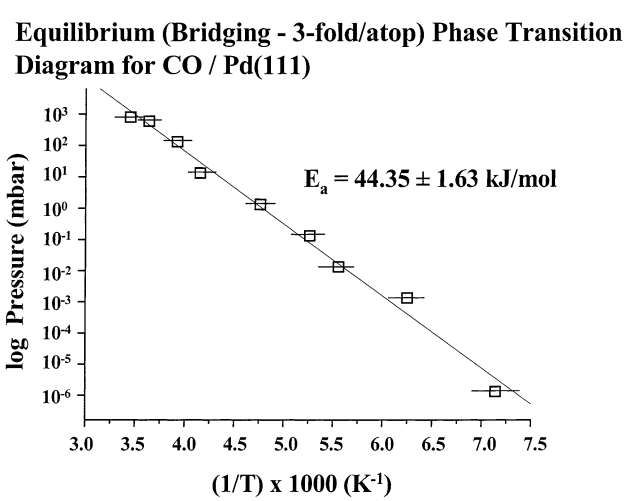

Figure 4. Isosteric plot for the phase transition from bridging to atop/3-fold CO on Pd(111).

IV. Conclusion

The adsorption of CO on a Pd(111) single-crystal surface was studied at quasi-atmospheric adsorbate pressures (800 mbar) between 225 and 650 K using the PM-IRAS technique. These experiments show the following: (a) The coverage-dependent CO overlayer structure follows the same trends in the 10^{-6}−800 mbar pressure regime, that is, no high-pressure species or adsorbate-induced substrate reconstructions are apparent. (b) The transition from an adsorbate superstructure dominated by the population of bridged sites to a different adsorbate overlayer having 3-fold/atop occupied sites was followed by varying the CO pressure over 9 orders of magnitude. The phase diagram was found to be in excellent agreement with previous results regarding the activation energy (44.35 ± 1.63 kJ/mol). (c) These results show a very strong correlation with recently published SFG data. Compared with SFG, PM-IRAS is relatively simple and has advantages regarding the versatility of investigating different spectral windows without using any other additional optical elements, quantitative information about various adsorbates, Lorentzian-like symmetric line shapes, and ambient optical elements. (d) PM-IRAS is a very versatile and a relatively simple spectroscopic technique regarding data acquisition and data analysis and is one that can be applied to a wide range of in situ catalytic problems at high-pressure and temperature conditions.

Acknowledgment. The authors acknowledge support from the Department of Energy, Office of Basic Energy Sciences, Division of Chemical Sciences, and the Robert A. Welch Foundation. The authors also are pleased to acknowledge Richard Jackson (Bruker, Inc.) for his help with the PM-IRAS setup and Christian Hess (Texas A&M University) for helpful discussions.

References and Notes

(1) Somorjai, G. *Introduction to Surface Chemistry and Catalysis*; John Wiley & Sons: New York, 1994.
(2) Goodman, D. W. *Chem. Rev.* **1995**, *95*, 523.
(3) Goodman, D. W. *J. Phys. Chem.* **1996**, *100*, 13090.
(4) Somorjai, G. A.; McCrea, K. R. *Adv. Catal.* **2000**, *45*, 385.

(5) Somorjai, G. A.; Rupprechter, G. *J. Phys. Chem. B* **1999**, *103*, 1623.
(6) Dellwig, T.; Rupprechter, G.; Unterhalt, H.; Freund, H. J. *Phys. Rev. Lett.* **2000**, *85*, 776.
(7) Dellwig, T.; Hartmann, J.; Libuda, J.; Meusel, I.; Rupprechter, G.; Unterhalt, H.; Freund, H. J. *J. Mol. Catal. A: Chem.* **2000**, *162*, 51.
(8) Green, M. J.; Barner, B. J.; Corn, R. M. *Rev. Sci. Instrum.* **1991**, *62*, 1426.
(9) Barner, B. J.; Green, M. J.; Saez, E. I.; Corn, R. M. *Anal. Chem.* **1991**, *63*, 55.
(10) Beitel, G. A.; Laskov, A.; Oosterbeek, H.; Kuipers, E. W. *J. Phys. Chem.* **1996**, *100*, 12494.
(11) Beitel, G. A.; deGroot, C. P. M.; Oosterbeek, H.; Wilson, J. H. *J. Phys. Chem. B* **1997**, *101*, 4035.
(12) Kunimatsu, K.; Golden, W. G.; Seki, H.; Philpott, M. R. *Langmuir* **1985**, *1*, 245.
(13) Blaudez, D.; Turlet, J. M.; Dufourcq, J.; Bard, D.; Buffeteau, T.; Desbat, B. *J. Chem. Soc., Faraday Trans.* **1996**, *92*, 525.
(14) Buffeteau, T.; Desbat, B.; Turlet, J. M. *Appl. Spectrosc.* **1991**, *45*, 380.
(15) Richmond, W. N.; Faguy, P. W.; Jackson, R. S.; Weibel, S. C. *Anal. Chem.* **1996**, *68*, 621.
(16) Kunimatsu, K.; Seki, H.; Golden, W. G.; Gordon, J. G.; Philpott, M. R. *Langmuir* **1988**, *4*, 337.
(17) Dunn, D. S.; Golden, W. G.; Severson, M. W.; Overend, J. *J. Phys. Chem.* **1980**, *84*, 336.
(18) Blaudez, D.; Buffeteau, T.; Cornut, J. C.; Desbat, B.; Escafre, N.; Pezolet, M.; Turlet, J. M. *Appl. Spectrosc.* **1993**, *47*, 869.
(19) Golden, W. G.; Kunimatsu, K.; Seki, H. *J. Phys. Chem.* **1984**, *88*, 1275.
(20) Faguy, P. W.; Richmond, W. N.; Jackson, R. S.; Weibel, S. C.; Ball, G.; Payer, J. H. *Appl. Spectrosc.* **1998**, *52*, 557.
(21) Hoffmann, F. M. *Surf. Sci. Rep.* **1983**, *3*, 107 and references therein.
(22) Kuhn, W. K.; Szanyi, J.; Goodman, D. W. *Surf. Sci.* **1992**, *274*, L611.
(23) Szanyi, J.; Kuhn, W. K.; Goodman, D. W. *J. Vac. Sci. Technol., A* **1993**, *11*, 1969.
(24) Szanyi, J.; Kuhn, W. K.; Goodman, D. W. *J. Phys. Chem.* **1994**, *98*, 2978.
(25) Ortega, A.; Hoffman, F. M.; Bradshaw, A. M. *Surf. Sci.* **1982**, *119*, 79.
(26) Meier, D.; Ozensoy, E.; Goodman, D. W., to be submitted for publication.
(27) Grunze, M.; Ruppender, H.; Elshazly, O. *J. Vac. Sci. Technol., A* **1988**, *6*, 1266.
(28) Giessel, T.; Schaff, O.; Hirschmugl, C. J.; Fernandez, V.; Schindler, K. M.; Theobald, A.; Bao, S.; Lindsay, R.; Berndt, W.; Bradshaw, A. M.; Baddeley, C.; Lee, A. F.; Lambert, R. M.; Woodruff, D. P. *Surf. Sci.* **1998**, *406*, 90.
(29) Bourguignon, B.; Carrez, S.; Dragnea, B.; Dubost, H. *Surf. Sci.* **1998**, *418*, 171.
(30) Unterhalt, H.; Rupprechter, G.; Freund, H. J. *J. Phys. Chem. B* **2002**, *106*, 356.
(31) Rupprechter, G.; Unterhalt, H.; Morkel, M.; Galletto, P.; Hu, L.; Freund, H. J. *Surf. Sci.* **2002**, *502*−*503*, 109.
(32) Rupprechter, G. *Phys. Chem. Chem. Phys.* **2001**, *3*, 4621.
(33) Woodruff, D. P.; Hayden, B. E.; Prince, K.; Bradshaw, A. M. *Surf. Sci.* **1982**, *123*, 397.